NUCL SCI TECH (2018) 29:103
https://doi.org/10.1007/s41365-018-0429-6

Monte Carlo simulation of incident electrons passing through thin metal layer

Tian-Long He[1] · Hong-Liang Xu[1] · Kai-Ting Huang[1] · Zhi-Liang Ren[1] · De-Rong Xu[1]

Received: 3 November 2017 / Revised: 5 December 2017 / Accepted: 26 December 2017 / Published online: 30 May 2018

Abstract A Monte Carlo simulation using two schemes, the discrete energy loss approach and the continuous slowing down approximation, was implemented in C++ to calculate the energy transmission coefficient and average energy loss for low-energy (1–10 keV) incident electrons passing through a thin metal layer. The simulation model uses the Ashley model for electron inelastic scattering, the electron elastic scattering cross section taken from the NIST database, and the stopping power derived from the full Penn algorithm. The results of the two schemes agree well with each other and can be used to quantitatively evaluate the shielding effect of a thin coated metal layer on incident electrons for a diamond amplified photocathode.

Keywords Monte Carlo simulation · Coated metal · Energy transmission coefficient · Average energy loss

1 Introduction

As a novel photoinjector design concept, the diamond amplified photocathode (DAP) was proposed to provide high-quality electron beams for new linac-based light sources such as the X-ray free-electron laser and energy-recovery linac [1–8]. Figure 1a shows the structure of the diamond window, an essential component of the DAP. The metal coating on the incident surface of the diamond film is usually 30–50 nm in thickness and acts as a negative electrode to drive secondary electrons (SEs) toward the emission surface. However, the metal coating will inevitably cause some energy loss of incident electrons.

As shown in Fig. 1b, the metal coating acts as a shield, and only transmitted electrons, including transmitted primary electrons and transmitted SEs, can enter the diamond to produce SEs by ionization. The ratio of the number of SEs generated in the diamond to the number of incident electrons is called the SE generation gain. To quantitatively evaluate the shielding effect of the metal coating on incident electrons, we denote the energy transmission coefficient and average energy loss of incident electrons as η_E and ΔE, respectively. These variables are described in detail in Sect. 2.6.

The Monte Carlo method is widely used in simulations of electron transport in solids [9–13]. Instead of studying the SE emission yield and energy distribution of backscattered electrons, we focus on the η_E and ΔE values of incident electrons. η_E and ΔE can be calculated using two simulation schemes: the discrete energy loss approach (DELA) and continuous slowing down approximation (CSDA) [12]. The main difference is that the DELA deals with the energy loss in discrete inelastic collisions, but the CSDA uses an approximation of continuity in describing the energy loss calculated using the stopping power.

Because Al, Ti, Pt, or Au can be used as the coating material for the DAP, in this work, we aim to calculate the η_E and ΔE values of incident electrons for these metals by varying the primary energy in the range of 1–10 keV and the thickness of the coated metal layer. The simulation details and results are presented in later sections.

This work was supported by the National Natural Science Foundation of China (No. 11375176).

✉ Hong-Liang Xu
hlxu@ustc.edu.cn

[1] National Synchrotron Radiation Laboratory, University of Science and Technology of China, Hefei 230029, China

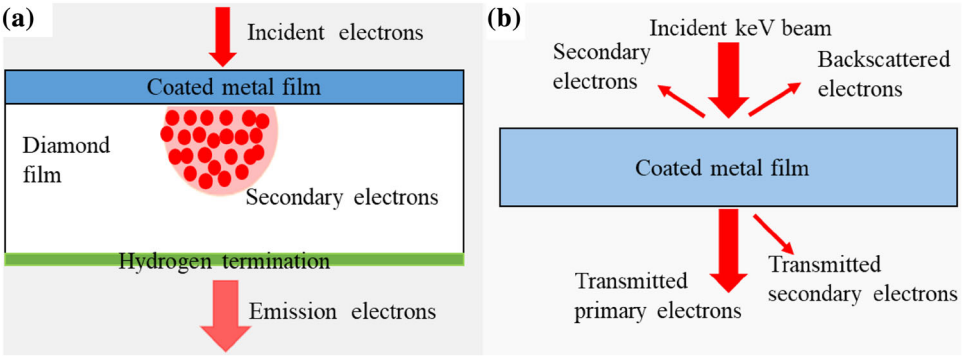

Fig. 1 (Color online) Schematic of diamond window structure (**a**) and the interaction of incident electrons with the coated metal film (**b**)

2 Theory and method

Considering that the total energy of transmitted electrons with energy < 50 eV is much less than that of transmitted electrons with energy > 50 eV, the cutoff energy can be set to 50 eV. We thus need to deal with the electron scattering process in the energy range of 50–10^4 eV. In this energy range, the Mott cross section is generally used to describe the electron elastic scattering, and a dielectric approach to electron inelastic scattering is used [9–13]. In this work, we used the differential elastic scattering cross sections (DCSs) taken from the NIST database [14]. The DCSs can be used to calculate the elastic mean free path and elastic scattering angle [10–12]. For inelastic collisions, the Ashley model based on the dielectric theory can be used to calculate the energy loss of primary electrons [15, 16]. The stopping power needed by the CSDA was calculated using the full Penn algorithm (FPA) model [17].

2.1 Mean free path

The elastic mean free path can be calculated using the total elastic cross section [9, 12]:

$$\lambda_{\mathrm{el}} = \frac{A}{\rho N_{\mathrm{A}} \sigma_{\mathrm{el}}}, \tag{1}$$

where λ_{el} is the elastic mean free path (in Å), A is the atomic weight, N_{A} is the Avogadro number, ρ is the density of the material (in g/Å^3), and σ_{el} is the total elastic cross section (in Å^2). σ_{el} can be obtained by integrating the differential cross section over the entire polar angle:

$$\sigma_{\mathrm{el}} = \int_0^{\pi} \frac{\mathrm{d}\sigma}{\mathrm{d}\theta} \mathrm{d}\theta, \tag{2}$$

where $\mathrm{d}\sigma/\mathrm{d}\theta$ is the differential cross section obtained from the NIST database [14].

The inelastic mean free path can be calculated using a modified form of the Bethe equation proposed by Tanuma et al. [18]:

$$\lambda_{\mathrm{in}} = \frac{E}{E_{\mathrm{p}}^2[\beta \ln(\gamma E) - C/E + D/E^2]}, \tag{3}$$

where λ_{in} is the inelastic mean free path (in Å), E is the electron energy (in eV), E_{p} is the bulk plasma energy (in eV), and β, γ, C, and D are fitted parameters. The values of these parameters were given in Ref. [18].

Then the total mean free path can be given by [11, 12]

$$\lambda_{\mathrm{t}}^{-1} = \lambda_{\mathrm{el}}^{-1} + \lambda_{\mathrm{in}}^{-1}. \tag{4}$$

2.2 Energy loss

Under the CSDA, the energy loss is calculated according to the stopping power and the step length between two elastic collisions [11, 12]:

$$W = s\left(-\frac{\mathrm{d}E}{\mathrm{d}s}\right)_{\mathrm{Penn}}, \tag{5}$$

where $(-\mathrm{d}E/\mathrm{d}s)_{\mathrm{Penn}}$ is the stopping power calculated using the FPA, as shown in Fig. 2.

The step length s is selected by choosing a uniform random number R in the range 0–1 via

$$s = -\lambda_{\mathrm{el}} \ln(R). \tag{6}$$

Under the DELA, the energy loss can be calculated using the differential inelastic mean free path:

$$\int_0^{W} \frac{\mathrm{d}\lambda_{\mathrm{in}}^{-1}}{\mathrm{d}w}\mathrm{d}w \Big/ \int_0^{W_{\max}} \frac{\mathrm{d}\lambda_{\mathrm{in}}^{-1}}{\mathrm{d}w}\mathrm{d}w = R, \tag{7}$$

where $W_{\max}$ is $3/4E$ according to the Ashley model [15, 16], W is the possible energy loss and is varied from 0 to $W_{\max}$, R is a random number, and the differential inelastic mean free path $\mathrm{d}\lambda_{\mathrm{in}}^{-1}/\mathrm{d}w$ can be expressed as

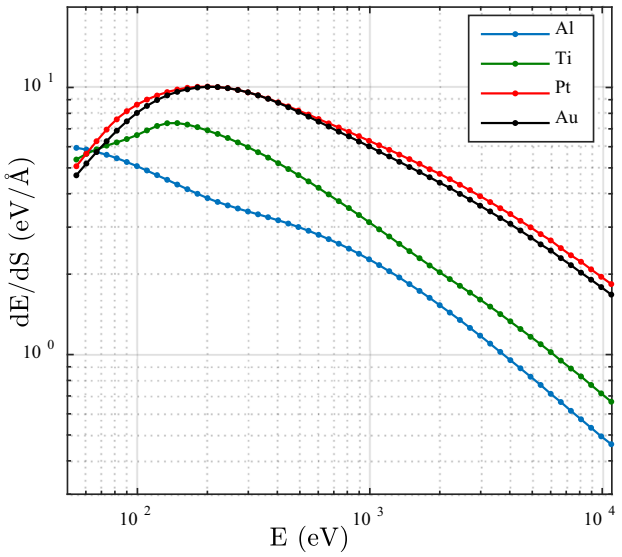

Fig. 2 (Color online) Stopping power of Al, Ti, Pt, and Au provided by Shinotsuka, et al. [17]

$$\frac{\mathrm{d}\lambda_{\mathrm{in}}^{-1}}{\mathrm{d}w} = \frac{1}{\pi a_0 E}\int_{q_-}^{q_+}\frac{\mathrm{d}q}{q}\mathrm{Im}\left[\frac{-1}{\varepsilon(q,w)}\right], \tag{8}$$

where a_0 is the Bohr radius, E is the initial energy of the primary electron, w is the energy loss, and q is the momentum transfer in the range of q_-–q_+. Further, $\hbar q_\pm = \sqrt{2mE} \pm \sqrt{2m(E-w)} \cdot \mathrm{Im}[-1/\varepsilon(q,w)]$ is the energy loss function, which can be obtained by extending the optical energy loss function $\mathrm{Im}[-1/\varepsilon(0,w)]$. In the Ashley model, it is given by

$$\mathrm{Im}[-1/\varepsilon(q,w)] = \int_0^\infty \mathrm{d}w_\mathrm{p}\frac{w_\mathrm{p}}{w}\delta\big(w - w_\mathrm{p}(q)\big)\mathrm{Im}[-1/\varepsilon(0,w)], \tag{9}$$

where w_p is the plasmon energy, and $w_\mathrm{p}(q)$ is given by

$$w_\mathrm{p}(q) = w_\mathrm{p} + \frac{\hbar^2 q^2}{2m}. \tag{10}$$

The optical energy loss functions of Al, Ti, Pt, and Au can be derived from handbooks of optical data [19, 20]. Equations 7–10 can be used to calculate the energy loss for inelastic collisions.

It is worth noting that Penn proposed another, more accurate, model, i.e., the FPA, to describe the inelastic scattering process [21, 22]. Shinotsuka et al. [17] have calculated the stopping power using the FPA model. We used the Ashley model to apply the DELA because it has a simpler expression formula than the FPA. In addition, we also used the stopping power based on the FPA to implement the CSDA.

2.3 Secondary electron generation

Energetic electrons propagating in solids lose energy owing to inelastic scattering, and the energy loss can excite an SE from the outer shell or core shell or cause plasmon excitation.

If an SE is excited owing to energy loss, we assume that the SE originated as a Fermi sea electron; then the initial energy of the SE can be calculated according to its excitation probability, which is proportional to the joint density of states of free electrons [23], i.e., $P(E',W) \propto \sqrt{E'(E'+W)}$ via

$$\int_0^{E_{\mathrm{s,ini}}} P(E',W)\mathrm{d}E' \Big/ \int_0^{E_\mathrm{F}} P(E',W)\mathrm{d}E' = R, \tag{11}$$

where $E'(E'<E_F)$ is the energy of a Fermi sea electron, W is the specific energy loss, $E_{\mathrm{s,\ ini}}$ is the initial energy of the SE, and R is a random number. The final energy of the SE can thus be given by $E_{\mathrm{s,\ ini}} + W$.

2.4 Scattering angle

Figure 3 shows the possible scattering process of an electron in a coated metal film, including elastic and inelastic scattering. To accurately trace its trajectory, the scattering angle, including the polar and azimuthal angles, should be known.

The polar elastic scattering angle can be calculated using the differential cross section:

$$\int_0^{\theta_\mathrm{Pe}} \frac{\mathrm{d}\sigma}{\mathrm{d}\theta}\mathrm{d}\theta \Big/ \int_0^{\pi} \frac{\mathrm{d}\sigma}{\mathrm{d}\theta}\mathrm{d}\theta = R, \tag{12}$$

where θ_Pe is the required polar elastic angle of primary electrons, and R is a random number.

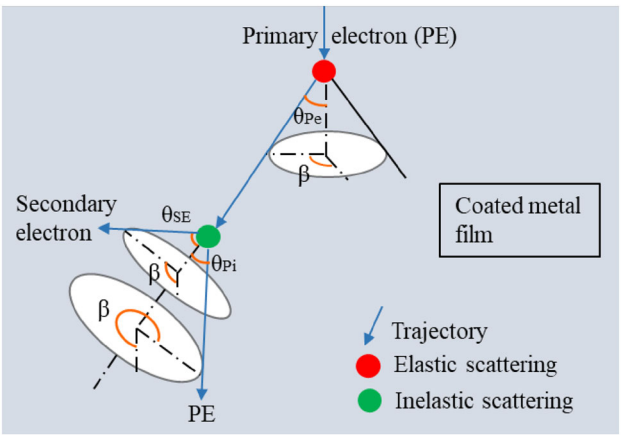

Fig. 3 (Color online) Schematic of electron scattering in coated metal

The polar inelastic scattering angle can be calculated by the Møller scattering angle formula [9, 24]:

$$\sin^2(\theta_{\mathrm{pi}}) = \frac{2E_{\mathrm{n}}}{2+\mu-\mu E_{\mathrm{n}}}, \tag{13}$$

$$\sin^2(\theta_{\mathrm{SE}}) = \frac{2-2E_{\mathrm{n}}}{2+\mu E_{\mathrm{n}}}, \tag{14}$$

where θ_{Pi} and θ_{SE} are the polar angles of primary electrons and SEs, respectively, during inelastic scattering; μ is the kinetic energy of the electron in units of its rest mass (511 keV); and E_{n} equals W/E, where W is the energy loss of the primary electrons, and E is the kinetic energy.

The azimuthal scattering angle including elastic and inelastic scattering can be calculated by

$$\beta = 2\pi R, \tag{15}$$

where R is a random number.

There is also another method to calculate the inelastic polar angle. Considering only SEs with energy exceeding 50 eV, which corresponds to a large energy loss W, the polar inelastic angle of primary electrons is just that predicted by the classical binary collision model [11, 12]:

$$\sin\theta_{\mathrm{Pi}} = (W/E)^{1/2}, \tag{16}$$

and the corresponding polar angle of SEs can be obtained assuming that SEs emerge with spherical symmetry [12, 25]:

$$\theta_{\mathrm{SE}} = \pi R. \tag{17}$$

We found that the difference between the results (η_{E} and ΔE) calculated using Eqs. 13, 14, 16, 17 is very small. In this work, Eqs. 13 and 14 were used to calculate the polar inelastic scattering angle.

2.5 Monte Carlo procedure

In the Monte Carlo simulation, for both the CSDA and DELA, the step length between two successive collisions must be computed first. For the CSDA, the step length $\boldsymbol{s}$ can be calculated using Eq. 6. Then the energy loss of primary electrons corresponding to this step length can be calculated using Eq. 5.

For the DELA, the step length $\boldsymbol{s}$ can be obtained using the total mean free path via

$$s = -\lambda_{\mathrm{t}}\ln(R). \tag{18}$$

After an electron passes the step length $\boldsymbol{s}$, the type of individual scattering event should be determined:if

$$R \le \lambda_{\mathrm{el}}^{-1}/\lambda_{\mathrm{t}}^{-1}, \tag{19}$$

it is elastic without any energy loss; otherwise, it is inelastic with the energy loss calculated using Eq. 7.

After collisions, the elastic scattering angle of primary electrons for both the CSDA and DELA can be calculated using Eq. 11, and the inelastic angle for the DELA can be calculated using Eqs. 13 and 14. Under the CSDA, SE generation is completely neglected, and only primary electrons are tracked. Under the DELA, two extreme conditions are considered: one is that SE generation is ignored, and the other is that every energy loss will excite an SE.

2.6 Calculation object

The number and energy of transmitted electrons are recorded. If their number is N_{t}, which corresponds to the total number N of incident electrons, their average energy can be calculated and is denoted by E_{ave}. The energy transmission coefficient is defined as the ratio of the total energy of transmitted electrons to the total energy of incident electrons and thus can be given by

$$\eta_{\mathrm{E}} = N_{\mathrm{t}}E_{\mathrm{ave}}/NE, \tag{20}$$

where $N_{\mathrm{t}}E_{\mathrm{ave}}$ and NE are the total energies of transmitted electrons and incident electrons, respectively. η_{E} can be used to evaluate the energy shielding effect of the coated metal film on incident electrons.

The average energy loss is defined as the ratio of the total energy loss ($NE - N_{\mathrm{t}}E_{\mathrm{ave}}$) to the total number N of incident electrons and can be given by

$$\Delta E = \frac{NE - N_{\mathrm{t}}E_{\mathrm{ave}}}{N} = E(1-\eta_{\mathrm{E}}). \tag{21}$$

ΔE can be used to analyze the reduction in the SE generation gain caused by the coated metal for a DAP. It is known that the energy required to create an electron–hole pair in diamond is E_{ion} = 13.4 eV [26, 27]; thus, the reduction in the gain can be given approximately by $\Delta E/E_{\mathrm{ion}}$.

3 Results and discussion

A Monte Carlo simulation was carried out under the CSDA and DELA for the following conditions: primary energies of 1–10 keV, thin coated metal films of Ti, Pt, or Au with thicknesses of 15–50 nm and of Al with thicknesses of 30–80 nm, and a cutoff energy of 50 eV. We found that tracing 5×10^5 electron trajectories was sufficient to reach a stable result.

3.1 Energy distribution

Figure 4 shows the energy distribution of transmitted electrons calculated under the DELA. On the left, the solid

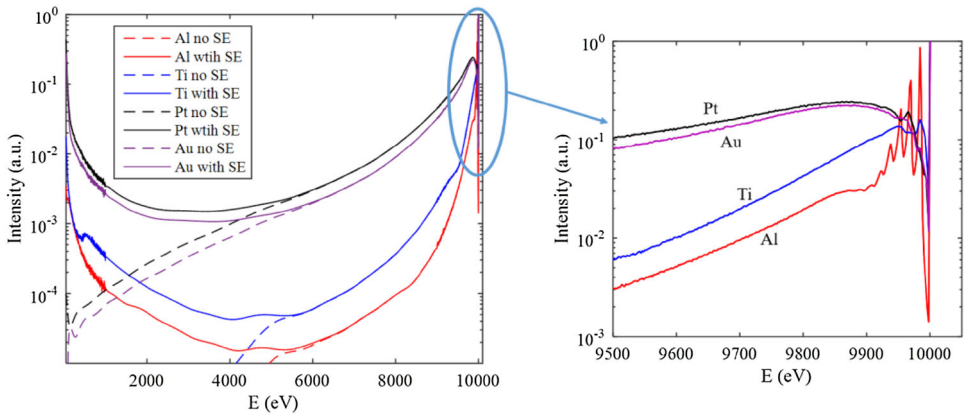

Fig. 4 (Color online) Energy distribution of transmitted electrons for 10 keV primary electrons passing through 30-nm-thick metal coating under DELA

curves correspond to the transmitted electrons, including secondary and primary electrons, whereas the dashed curves correspond only to transmitted primary electrons. In the 1–9 keV range, the calculated results fluctuate greatly because fewer electrons are counted in this energy range. Therefore, the fitted results are given and are reflected in the smooth shape of these curves in the 1–9 keV range. In the 7–10 keV range, the solid and dashed curves coincide.

The area surrounded by an ellipse in the left panel was enlarged, as shown in the right panel. The common feature of these four curves is that the highest peak is located at 10 keV and corresponds to transmitted primary electrons without inelastic scattering. The energy distribution of Al is apparently different from that of the other three metals; i.e., there are several peaks distributed in the 9.9–10 keV range, and the interval between peaks is about 15 eV. This feature coincides with the plasmon energy of $\sim$ 15 eV in Al, confirming that the chief energy loss mechanism in Al is plasmon excitation. We can also see that, for Pt and Au, a large number of the transmitted electrons appear in a wider energy range (7–10 keV). However, for Ti and Al, the transmitted electron energy distribution range is relatively concentrated at 9.5–10 keV.

3.2 Energy transmission coefficient

Figure 5 shows the energy transmission coefficient calculated using Eq. 20 under the DELA. In Fig. 5, the solid curve shows the results when SE generation is considered, and the dashed curve shows the results when SE generation is neglected. We can see that the two curves are very close, although the results with SE generation are slightly higher than those without SE generation. This result confirms that primary electrons make the dominant contribution to the total energy of transmitted electrons. Considering that the actual result is larger than the calculated result when SE generation is neglected but lower than that in the extreme case considering SE generation, the average value of both results is taken as the suggested result under the DELA. This suggested result should be very close to the actual result and will be compared with the calculated result under the CSDA.

Figure 6 shows the energy transmission coefficients, where the solid curves are the results calculated under the CSDA, and the dashed curves are the suggested results under the DELA. Curves of different color represent metal films of different thickness. Three thicknesses, 30, 50, and 80 nm, were chosen for the calculation for Al, but thicknesses of 15, 30, and 50 nm were chosen for Ti, Pt, and Au.

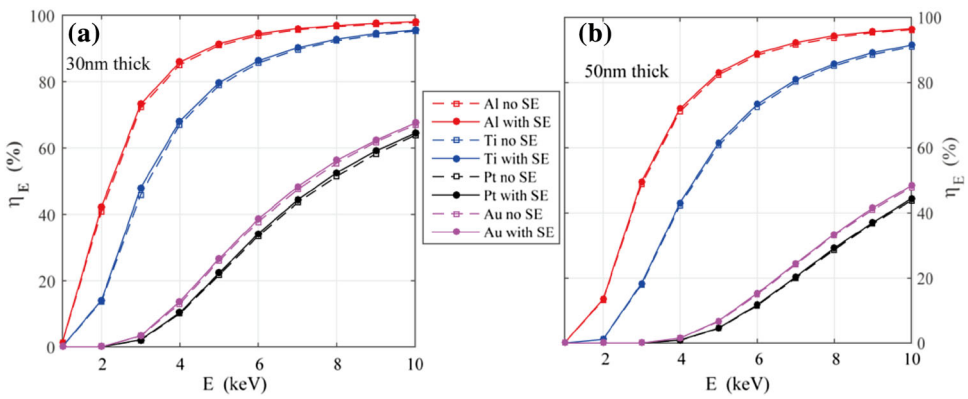

Fig. 5 (Color online) Energy transmission coefficient under DELA for metal film in thickness of 30 nm (**a**) and 50 nm (**b**)

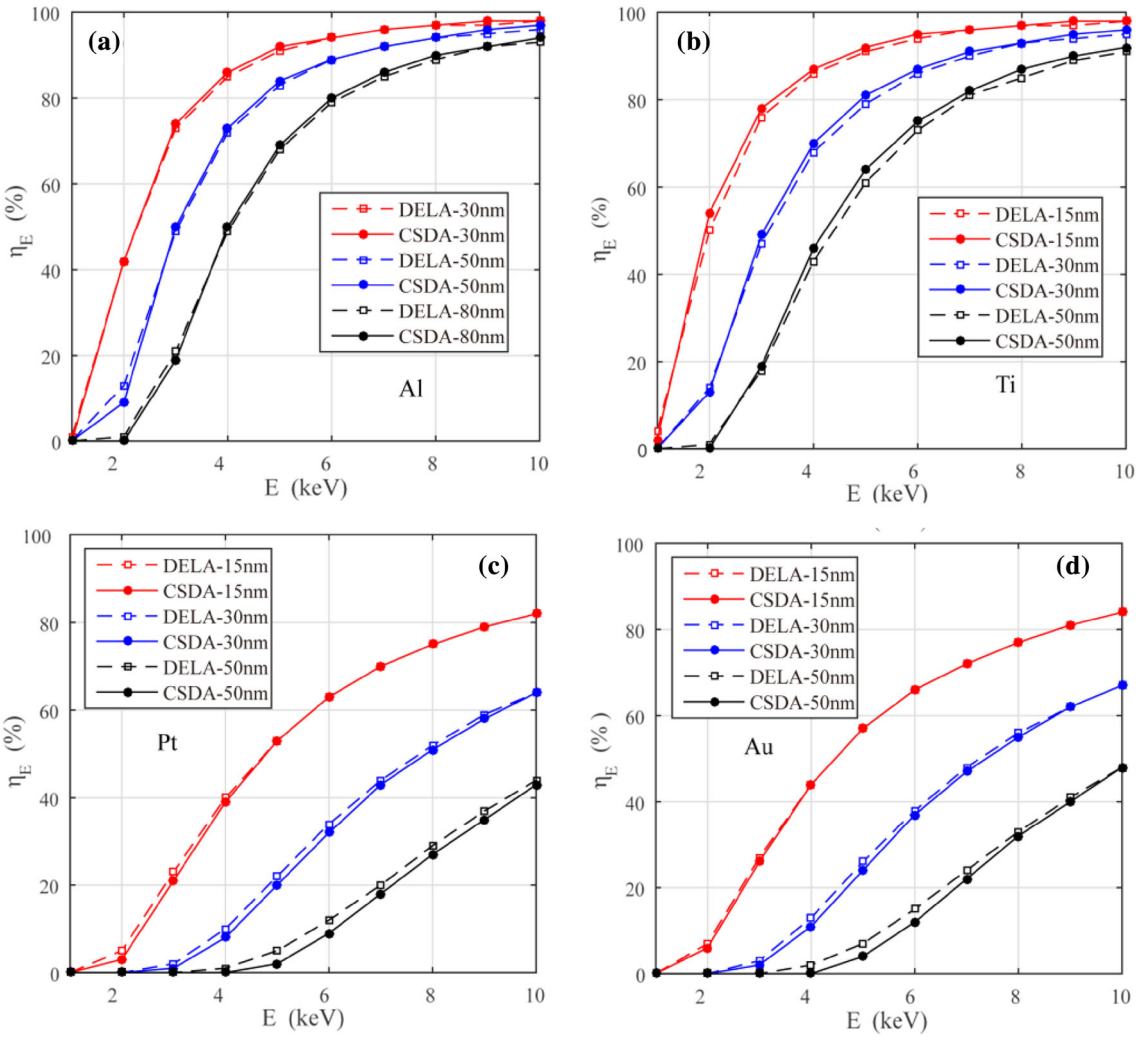

Fig. 6 (Color online) Energy transmission coefficient for metal films of Al (**a**), Ti (**b**), Pt (**c**), and Au (**d**)

First, it can be seen that for Al and Ti, the results of the CSDA are slightly higher than those of the DELA, and for Pt and Au, the results of the CSDA are slightly lower than those of the DELA. Then, according to the shape of the curves, it is obvious that for thinner metal coatings and higher incident electron energies, the energy transmission coefficient increases. As heavy metals, Pt and Au have a much stronger shielding effect on the incident electrons than Al and Ti. According to the results shown in Fig. 6, for an incident energy of 10 keV and a coating thickness of 30 nm, the energy transmission coefficient is 98, 95, 64, and 67% for Al, Ti, Pt, and Au, respectively.

There is a threshold energy for the energy transmission coefficient. For 80-nm-thick Al and 50-nm-thick Ti, the threshold energy is at least 2 keV, which means that incident electrons would be totally shielded if their primary energy was lower than 2 keV. For 30-nm-thick Pt and Au, the threshold energy is in the range of 2–3 keV, but is close to 3 keV. Although the threshold energy was discussed only in an approximate range here, it is worth noting that the actual value of the threshold energy can be calculated using our program.

3.3 Average energy loss

To conveniently evaluate the reducing effect of the metal coating on the SE generation gain of a DAP, it is better to give the average energy loss computed using Eq. 21; e.g., if the average energy loss was 3 keV, then the reduction in the SE generation gain can be given approximately by 3000/13.4 = 224.

Figure 7 shows the average energy loss calculated using the energy transmission coefficient results shown in Fig. 6. For an incident energy of 10 keV and a coating thickness of 30 nm, the average energy loss calculated under the CSDA is approximately 180, 430, 3610, and 3290 eV for Al, Ti, Pt, and Au, respectively, and the corresponding

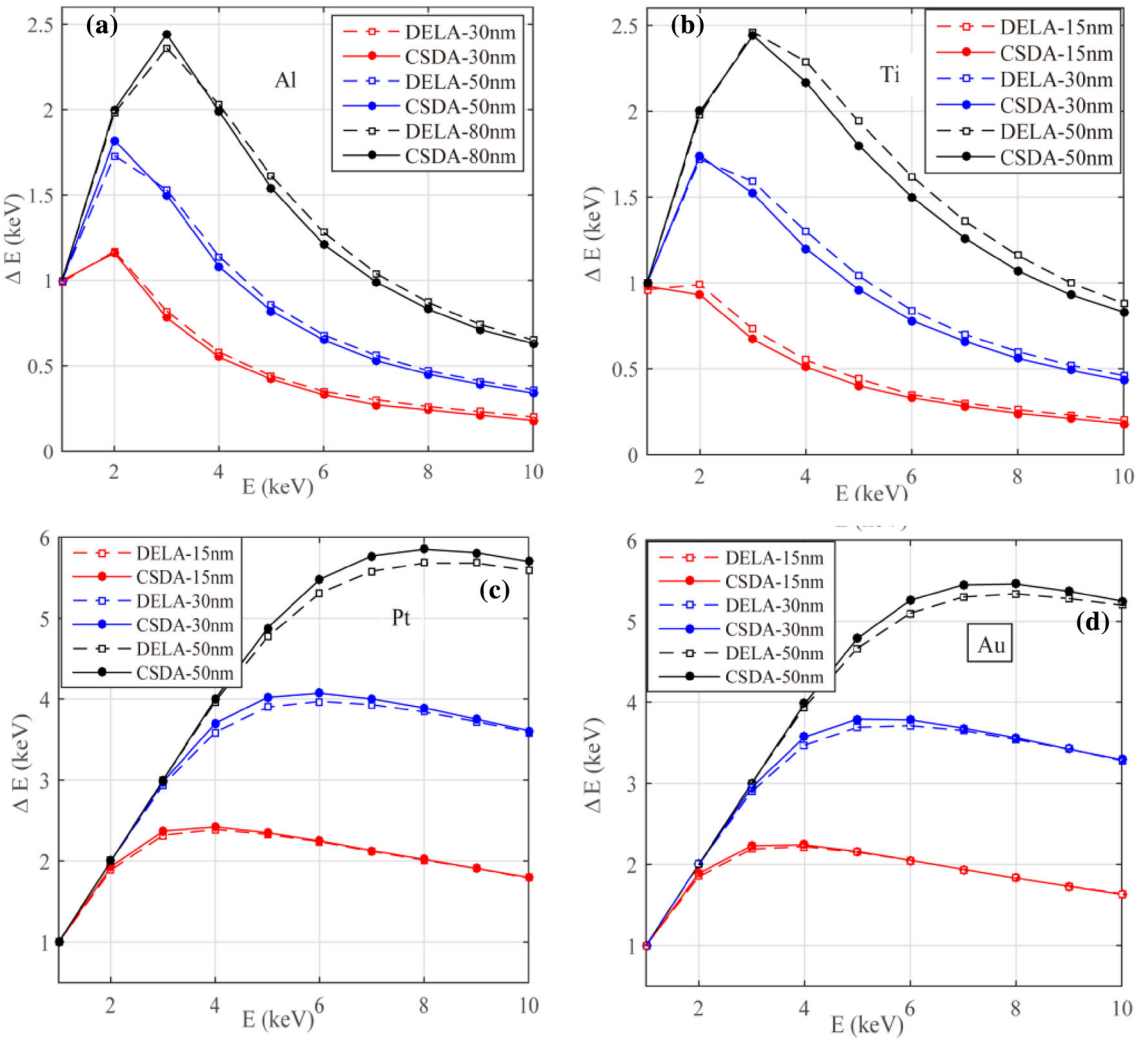

Fig. 7 (Color online) Average energy loss for metal films of Al (**a**), Ti (**b**), Pt (**c**), and Au (**d**) The solid curve corresponds to the CSDA, and the dashed curve corresponds to the DELA

reduction in the SE generation gain is approximately 13, 32, 269, and 246 for Al Ti Pt Au, respectively.

3.4 Error analysis

To reduce the calculation's systematic error caused by the Monte Carlo method itself, the number of tracked primary electrons was set to 5×10^5 for the DELA and CSDA, which is sufficient to reach stable results.

It should be noted that the correctness of the calculation results depends on the accuracy of the calculation model. We use a simplified treatment for the calculation model under the CSDA and DELA, i.e., by completely ignoring SE generation for the CSDA and considering two extreme cases, as mentioned above, for the DELA, and by setting the energy cutoff to 50 eV. Although this treatment will introduce some error, it still works well because the transmitted primary electrons make the dominant contribution to the total energy of transmitted electrons.

It can be observed from Fig. 7 that there are errors between the ΔE values calculated under the CSDA and DELA. Figure 8 compares the errors of the ΔE values calculated under the DELA and under the CSDA. The maximum relative error of ΔE is 14% for Al and 9% for Ti, but it is 3% for Pt and Au. The error comes mainly from the difference between the two optical models, i.e., the Ashley model and FPA model, used in the DELA and CSDA, respectively.

It is shown that although two different schemes (the DELA and CSDA) were employed in the calculation, and each scheme is based on different calculation models, the difference between the two types of results is acceptably small.

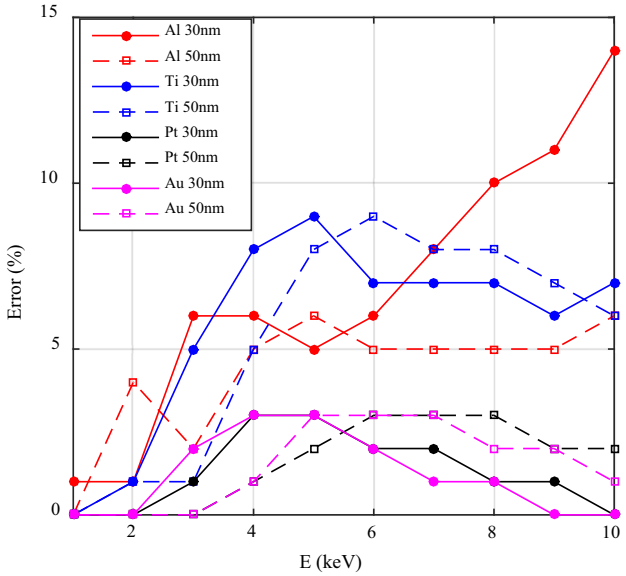

Fig. 8 (Color online) Error of the average energy loss ΔE under the DELA relative to that under the CSDA

4 Conclusion

We implemented a Monte Carlo simulation of electron transport in metal films using the DELA and CSDA to study quantitatively the shielding effect of a coated metal film on incident electrons for a DAP without considering the details of SE generation. It is valid in the energy range of 50–10^4 eV. The energy transmission coefficient and average energy loss of incident electrons calculated under the DELA and CSDA are close to each other, and the error between them is acceptable. We observed quantitatively that the heavy metals Pt and Au cause a much stronger shielding effect than the light metals Al and Ti. The results show that if 30-nm-thick Pt was used as the metal coating for a DAP, the average energy loss would be 3.61 keV for an incident electron energy of 10 keV, resulting in a reduction of the SE generation gain by approximately 269. This should be improved by changing the metal coating from one with complete coverage to a lithographically patterned grid coating. However, for 30-nm-thick Al and Ti, the average energy loss is small; thus, there is no need to consider using a lithographically patterned grid coating to reduce the average energy loss.

In addition to calculating the energy transmission coefficient and average energy loss, our program can also be used to study the backscattering coefficients (the DELA and CSDA), the energy distribution of backscattered electrons (the DELA), and the maximum incident range (the DELA and CSDA). However, it cannot be used to analyze the SE emission yield because it neglects the details of SE generation and sets the cutoff energy at 50 eV. This can be improved in future work.

References

1. J. Smedley, I. Ben-Zvi, A. Burrill et al., Electron amplification in diamond. AIP Conf. Proc. **877**, 672–679 (2006). https://doi.org/10.1063/1.2409200
2. X. Chang, Q. Wu, I. Ben-Zvi et al., Electron beam emission from a diamond-amplifier cathode. Phys. Rev. Lett. **105**, 164801 (2010). https://doi.org/10.1103/PhysRevLett.105.164801
3. X. Chang, *Studies in Laser Photo-cathode RF Guns* (Stoney Brook University, Stoney Brook, 2005)
4. X. Chang, I. Ben-Zvi, A. Burrill, et al., Study of secondary emission enhanced photoinjector, in *Proceeding of PAC05, Knoxville*, Tennessee, May 16–20 (2005)
5. D.A. Dimitrov, R. Busby, D.L. Bruhwiler, et al., 3D simulations of secondary electron generation and transport in a diamond amplifier for photocathodes, in *Proceeding of PAC07, New Mexico*, USA, June 25–29(2007)
6. D.A. Dimitrov, R. Busby, J.R. Cary et al., Multiscale three-dimensional simulations of charge gain and transport in diamond. J. Appl. Phys. **108**, 073712 (2010). https://doi.org/10.1063/1.3491041
7. E. Wang, I. Ben-Zvi, T. Rao, et al., Progress on diamond amplified photo-cathode, in *Proceeding of PAC2012*, New Orleans, Louisiana, USA, May 20–25 (2012)
8. T. Xin, S. Belomestnykh, I. Ben-Zvi, et al., Diamond amplifier design and preliminary test results, in *Proceeding of PAC2013,* Pasadena, CA, USA, 29 September–4 October (2013)
9. M.K. Alam, A. Nojeh, Monte Carlo simulation of electron scattering and secondary electron emission in individual multiwalled carbon nanotubes: a discrete-energy-loss approach. J. Vac. Sci. Technol., B **29**, 041803 (2011). https://doi.org/10.1116/1.3605300
10. Z.J. Ding, X.D. Tang, H.M. Li, Monte Carlo calculation of the energy distribution of backscattered electrons. Int. J. Mod. Phys. B **16**, 4405–4412 (2002). https://doi.org/10.1142/S0217979202015509
11. Z.J. Ding, R. Shimizu, A Monte Carlo modeling of electron interaction with solids including cascade secondary electron production. Scanning **18**, 92–113 (1996). https://doi.org/10.1002/sca.1996.4950180204
12. M. Dapor, *Transport of energetic electrons in solids* (Springer, Berlin, 2013), pp. 1–54
13. P. Xiao, The Monte Carlo simulation of secondary electrons excitation in the resist PMMA. Appl. Phys. Res. **6**, 3 (2014). https://doi.org/10.5539/apr.v6n3p1
14. F. Salvat, A. Jablonski, C.J. Powell, et al., NIST Electron Elastic-Scattering Cross-Section Database Version 4.0. NIST Standard Reference Database Number 64. (National Institute of Standards and Technology, Gaithersburg, 20899, 2016). https://srdata.nist.gov/SRD64/Elastic. Accessed 20 May 2017
15. J.C. Ashley, Interaction of low-energy electrons with condensed matter: stopping powers and inelastic mean free paths from optical data. J. Electron Spectrosc. Relat. Phenom. **46**, 199–214 (1988). https://doi.org/10.1016/0368-2048(88)80019-7
16. J.C. Ashley, Energy-loss probabilities for electrons, positrons, and protons in condensed matter. J. Appl. Phys. **69**, 674–678 (1991). https://doi.org/10.1063/1.347348
17. H. Shinotsuka, S. Tanuma, C.J. Powell et al., Calculations of electron stopping powers for 41 elemental solids over the 50 eV

to 30 keV range with the full Penn algorithm. Nucl. Instrum. Methods Phys. Res. B **270**, 75–92 (2012). https://doi.org/10.1016/j.nimb.2011.09.016
18. S. Tanuma, C.J. Powell, D.R. Penn, Calculations of electron inelastic mean free paths. IX. Data for 41 elemental solids over the 50 eV to 30 keV range. Surf. Interface Anal. **43**, 689–713 (2010). https://doi.org/10.1002/sia.3522
19. E.D. Palik, *Handbook of Optical Constants of Solids* (Academic Press, New York, 1985), pp. 290–405
20. E.D. Palik, *Handbook of Optical Constants of Solids III* (Academic Press, New York, 1998), pp. 243–247
21. S. Tanuma, C.J. Powell, D.R. Penn, Calculations of electron inelastic mean free paths for 31 materials. Surf. Interface Anal. **11**, 577 (1988). https://doi.org/10.1002/sia.740111107
22. D.R. Penn, Electron mean-free-path calculations using a model dielectric function. Phys. Rev. B **35**, 482 (1987). https://doi.org/10.1103/PhysRevB.35.482
23. S.F. Mao, Y.G. Li, R.G. Zeng et al., Electron inelastic scattering and secondary electron emission calculated without the single pole approximation. J. Appl. Phys. **104**, 114907 (2008). https://doi.org/10.1063/1.3033564
24. L.N. Pandey, M.L. Rustgi, A comparative study of electron transport phenomenon in the keV range. J. Appl. Phys. **66**, 6059–6064 (1989). https://doi.org/10.1063/1.343585
25. R. Shimizu, Z.J. Ding, Monte Carlo modelling of electron–solid interactions. Rep. Prog. Phys. **55**, 487–531 (1992)
26. B. Ziaja, R.A. London, J. Hajdu, Ionization by impact electrons in solids: Electron mean free path fitted over a wide energy range. J. Appl. Phys. **99**, 033514 (2006). https://doi.org/10.1063/1.2161821
27. J.W. Keister, J. Smedley, Single crystal diamond photodiode for soft X-ray radiometry. Nucl. Instrum. Methods Phys. Res., Sect. A **606**, 704–779 (2009). https://doi.org/10.1016/j.nima.2009.04.044